NH3 and O2 Interaction with Tetrahedral Ti3+ Ions Isomorphously Substituted in the Framework of TiAlPO-5. A Combined Pulse EPR, Pulse ENDOR, UV-Vis and FT-IR Study

UNIVERSITÀ DEGLI STUDI DI TORINO

NH_3 and O_2 Interaction with Tetrahedral Ti^{3+} Ions Isomorphously Substituted in the Framework of TiAlPO-5. A Combined Pulse EPR, Pulse ENDOR, UV-Vis and FT-IR Study.

Sara Maurelli,[a] Muthusamy Vishnuvarthan,[a,b] Gloria Berlier [a] and Mario Chiesa [a*]

Continuous Wave (CW), pulse Electron Paramagnetic Resonance (EPR) and pulse Electron Nuclear Double Resonance (ENDOR) spectroscopies, in conjunction with UV-Vis and Infra Red (IR) spectroscopies are used to investigate the chemical reactivity of tetrahedrally coordinated Ti^{3+} ions isomorphously substituted in the framework of AlPO-5 towards NH_3 and O_2. The coordination of ammonia to Ti^{3+} centres is followed in detail by complementary vibrational and electron magnetic resonance techniques. In particular HYSCORE spectra allow identifying the coordination of two ammonia molecules to Ti^{3+} centres resolving the full hyperfine and quadrupole ^{14}N coupling tensors. The reactivity of the reduced TiAlPO sample towards molecular oxygen is detailed by means of CW-EPR and pulse ENDOR spectroscopy. $^{17}O_2$ is employed, allowing to establish the formation of a "side-on" η^2 O_2^--Ti^{4+} electrostatic complex. Pulse ENDOR spectra provide detailed information on the local environment of the formed superoxide radical anion which acts as a paramagnetic probe, providing evidence for Ti-O-Ti oligomeric species.

1. Introduction

After the discovery of titanium-substituted silicalite-1 (TS-1),[1] with its remarkable catalytic properties, titanium insertion in tetrahedral sites of open framework materials has been pursued with the aim of obtaining new materials showing specific catalytic properties in selective oxidation reactions.[2,3] As an example, Ti insertion in the mesoporous structure of MCM-41 led to highly active and selective catalysts in different oxidation reactions, whereby the catalytic activity is associated to coordinatively unsaturated tetrahedral Ti(IV) ions, interacting with the reactants by expanding their coordination from four-fold up to six-fold.[4,5,6,7,8]

Before the discovery of TS-1, four-fold coordinated Ti compounds were considered very scarce, due to the strong tendency of the metal to adopt octahedral geometries.[9] As a consequence, the structure and chemistry of framework Ti^{4+} ions in TS-1,[10] or in mesoporous Ti-MCM-41[11,12] has been the subject of several experimental,[6,7,12,13] computational[14,15] and combined experimental/computational[11,16] studies, showing the reversible changes of the metal coordination in the presence of ligands or of H_2O_2 aqueous solutions.

Aluminophosphates AlPO-*n*, where *n* denotes a particular structure type, form a class of microporous crystalline materials comparable to the well-known zeolites and characterized by neutral lattices constituted by alternating PO_4 and AlO_4 tetrahedra.[17] AlPO's represent thus another class of open framework materials where isolated tetrahedral Ti sites can be obtained through isomorphous substitution and which are particularly interesting due to their specific activity towards different chemical processes.[18,19] Titanium incorporation into the aluminophosphate structure is of crucial importance in order to achieve significant catalytic performances, but actual incorporation into the tetrahedral framework is difficult to prove.

We have recently reported direct spectroscopic evidence, using Continuous Wave Electron Paramagnetic Resonance (CW-EPR) and Hyperfine Sublevel Correlation (HYSCORE) spectroscopies, for framework substitution of Ti in AlPO-5, an aluminophosphate zeotype with AFI structure.[20]

The oxidation-reduction behaviour of TiAlPO represents an important issue, which can be tackeled in a detailed way by means of EPR spectroscopy. Infact, while Ti(IV) ions are EPR silent, Ti^{3+} is characterized by a d^1 electron configuartion (S=1/2) and characteristic CW-EPR spectra, whose features strongly depend on the cation local symmetry. Moreover, in the case of AlPO materials, the paramagnetic species (Ti^{3+}) is surrounded by distinct magnetically active nuclei: ^{31}P (I=1/2) and ^{27}Al (I=5/2). The combination of conventional CW-EPR and HYSCORE spectroscopy allowed us to probe in detail the close environment of Ti^{3+} ions. In particular observation of large ^{31}P hyperfine couplings, combined with the absence of specific ^{27}Al couplings, provided direct evidence for framework substitution of redox active Ti ions at Al^{3+} sites.[20]

In this work we further explore the chemistry of Ti ions substituted in the AlPO-5 framework monitoring by combined CW and Pulse EPR and Pulse Electron Nuclear Double Resonance (ENDOR), complemented by DR-UV-Vis and FT-IR spectroscopies, the reactivity of reduced TiAlPO-5 towards ammonia and molecular oxygen.

2. Experimental Section

2.1 Sample preparation

TiAlPO-5 was prepared by hydrothermal synthesis by employing aluminum oxide hydroxide (Catapal B Alumina, Sasol), titanium isopropoxide (Aldrich), phosphoric acid (Sigma-Aldrich) and triethylamine (TEA, Sigma-Aldrich), resulting in a gel composition 0.1 TiO_2: 1 TEA: 1 Al_2O_3: 1 P_2O_5: 40 H_2O. After hydrothermal treatment at 448 K, the autoclave was cooled to room temperature and the solid product was washed, filtered and dried in air. Finally the product was calcined by heating until 823 K in a flow of nitrogen and kept at the same temperature in oxygen for 12 hours.

Calcined samples were dehydrated in vacuum by gradually raising the temperature to 673 K over a period of 2h and kept at that temperature for 1h. The dehydrated samples were then reduced under 100 Torr of H_2 at 723 K. Quantitative evaluation of the number of Ti(III) ions present in the sample was obtained by comparison of the CW-EPR absorption area with that of a solution of copper acetylacetonate of known concentration. High purity NH_3, O_2 and $^{17}O_2$ (90% ^{17}O enrichment, Aldrich) were used. NH_3 was purified by the freeze-thaw-pump method.

2.2 Characterization

X-band CW EPR spectra were detected at 77K on a Bruker EMX spectrometer (microwave frequency 9.75 GHz) equipped with a cylindrical cavity. A microwave power of 10 mW, modulation amplitude of 0.3 mT and a modulation frequency of 100 KHz was used.

Pulse EPR experiments were performed on an ELEXYS 580 Bruker spectrometer (at the microwave frequency of 9.76 GHz) equipped with a liquid-helium cryostat from Oxford Inc. All experiments were performed at 5 K. The magnetic field was measured by means of a Bruker ER035M NMR gauss meter.

Electron-spin-echo (ESE) detected EPR experiments were carried out with the pulse sequence: $\pi/2-\tau-\pi-\tau-echo$, with microwave pulse lengths $t_{\pi/2}$ = 16 ns and t_π = 32 ns and a τ value of 180 ns.

Davies ENDOR spectra were measured with the mw pulse sequence π-*T*-$\pi/2$-τ-π-τ-*echo*, with mw pulses of length $t_{\pi/2}$ = 300 ns and t_π = 600 ns, and τ = 1400 ns. A radio frequency pulse was applied during time *T*. The length of the radiofrequency π pulse was optimized for the two different nuclei (^{31}P and ^{1}H) by a nutation experiment. Optimal lengths were found to be 15 μs and 10.5 μs for ^{31}P and ^{1}H respectively.

Mims ENDOR spectra were measured with the mw pulse sequence $\pi/2$-τ-$\pi/2$-*T*-$\pi/2$-τ-*echo* with $t_{\pi/2}$ = 16 ns. In order to remove blind spots effects time τ was increased in steps of 8 ns from 96 ns to 256 ns and the spectra added together.

Hyperfine Sublevel Correlation (HYSCORE) experiments[21] were carried out with the pulse sequence $\pi/2-\tau-\pi/2-t_1-\pi-t_2-\pi/2-\tau-echo$ with the microwave pulse length $t_{\pi/2}$ = 16 ns and t_π = 16 ns. The time intervals t_1 and t_2 were varied in steps of 8 ns starting from 96 ns to 2704 ns. In order to avoid blind spot effects different τ values were chosen, which are specified in the figure captions. An eight-step phase cycle was used for eliminating unwanted echoes. The time traces of the HYSCORE spectra were baseline corrected with a third-order polynomial, apodized with a Hamming window and zero filled.

After two-dimensional Fourier transformation, the absolute value spectra were calculated. The spectra were added for the different τ values in order to eliminate blind-spot effects. Spectra were simulated using the Easyspin program.[22]

Diffuse Reflectance (DR) UV-Vis-NIR measurements were performed at room temperature (RT) on powdered samples by using a Perkin-Elmer (Lambda 19) spectrometer equipped with an integrating sphere using $BaSO_4$ as reference. Spectra were recorded in the 200 – 2500 nm range at a scan rate of 240 nm/min with a step size of 1 nm and slit opening of 4 mm. The measured intensities were converted with Kubelka-Munk function.

FTIR measurements were recorded on Bruker IFS 88 spectrometer with an DTGS detector, working with resolution of 4 cm^{-1} over 64 scans. Samples, in the form of self-supporting pellets suitable for transmission IR experiments, were directly treated in a quartz cell equipped with KBr windows, designed for RT studies in controlled atmosphere. Spectra were recorded by gradually increasing the ammonia equilibrium pressure (PNH_3) and, after checking the time evolution of the system, by step wise reduction PNH_3. The catalyst spectrum collected before gas dosage was used as reference for obtaining the reported background-subtracted spectra.

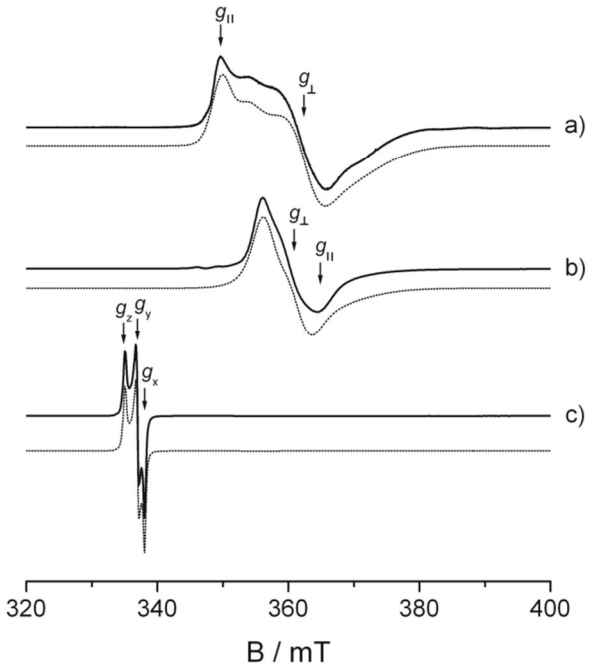

Fig. 1 Experimental (black line) and simulated (dotted line) CW EPR spectra of TiAlPO-5 upon (a) reduction in H_2 at 723K, (b) adsorption of 20 mbar of NH_3 and (c) adsorption of 1 mbar of O_2. All spectra were recorded at 77K. The arrows indicate the magnetic field positions at which HYSCORE and ENDOR experiments were performed.

Inductively Coupled Plasma – Atomic Emission (ICP-AES) measurements were performed with an Optima 7000 DV Perkin Elmer Spectrometer, equipped with a CCD detector (λ = 334.941 nm), in order to determine the total amount of Ti ions in the calcined sample. Sample treatment and analysis were carried out in triplicate. The relative standard deviations of the results were within 5%. Aliquots of 15 mg were treated with 3 ml of concentrated nitric acid. Calibrations were performed with standard solutions prepared in aliquots of sample blanks.

3. Results and discussion.

The as prepared TiAlPO-5 sample is EPR silent. Upon reduction with H_2 an EPR spectrum, characterized by a nearly axial **g** tensor, is given rise, which is due to the formation of Ti^{3+} ions. A typical spectrum is shown in Fig. 1a together with the corresponding computer simulation (dotted line). The experimental spectral pattern is the result of two overlapping species with nearly axial **g**-tensor components (Table 1). The *g* values of both species are typical for Ti^{3+} in a tetrahedral crystal field as in the case of tetrahedral titanium in TS-1[23] or in TiMCM-41.[24] Consistent with this evidence is the UV-Vis spectrum of the reduced sample (Fig. 2, dotted line), which shows a broad absorption band centered at about 870 nm (11500 cm^{-1}), consistent with the presence of Ti^{3+} species in tetrahedral coordination (see below).[20,25]

In a tetragonally distorted tetrahedral field, the *g* values calculated[26] to first order are, for tetragonal compression and elongation respectively:

$$g_{||} = g_e \text{ and } g_{\perp} = g_e - 6\lambda/\Delta \qquad (1)$$

and

$$g_{||} = g_e - 8\lambda/\Delta \text{ and } g_{\perp} = g_e - 2\lambda/\Delta \qquad (2)$$

where λ is the Ti spin orbit coupling constant and Δ the splitting between the e_g levels due to tetragonal distorsion. Using the values for λ = 154 cm^{-1}, and Δ = 11500 cm^{-1} obtained from the UV-Vis spectrum, the theoretical values $g_{||}$ = 2.0023 and $g_{\perp}$= 1.922 are obtained for the tetragonal compression case, while $g_{||}$= 1.895 and $g_{\perp}$=1.975 are obtained for the elongate distorsion.

Comparison with the experimental values ($g_z = g_{||}$ and $g_x \cong g_y = g_{\perp}$ in Table 1) clearly points to tetragonal compression as the most likely situation. Clear evidence of isomorphous substitution at Al^{3+} sites has been provided by HYSCORE spectroscopy, which allowed detecting ^{31}P hyperfine interactions typical for Ti-O-P coordination.[20] The reader is referred to reference 20 for the details, in the following we focus on the chemical reactivity of these Ti^{3+} framework species towards ammonia and molecular oxygen.

3.1 Chemical reactivity of TiAlPO-5 with NH_3

On reacting the sample with NH_3 dramatic changes in both EPR and UV-Vis spectra are observed. The CW-EPR spectrum observed upon NH_3 adsorption on the reduced TiAlPO-5 sample is shown in Fig. 1b. As already observed for H_2O adsorption,[20] the coordination of the Lewis base to Ti^{3+} centres is reflected in the change of the ***g*** tensor of the CW EPR spectrum, which is

characterized by a reversed symmetry ($g_{\|} < g_{\perp}$) with respect to the reduced sample ($g_{\|} > g_{\perp}$). Notice that upon ammonia adsorption the site heterogeneity observed in the reduced sample (Fig. 1a) is reduced and the spectrum can be simulated by considering a single species characterized by the spin Hamiltonian parameters reported in Table 1. This indicates that ammonia adsorbs unselectively on the different Ti^{3+} sites leading to similar local environments. The change in the ***g*** tensor is brought about by the ammonia adsorption and clearly indicates a change in the local crystal field as it may be expected and as already observed in the case of water coordination.[20] In both cases (H_2O and NH_3) the g factors are typical of Ti^{3+} in distorted octahedral symmetry and consistent with the unpaired electron mainly residing in either d_{xy} or d_{x2-y2} orbitals of Ti^{3+}. The original spectrum (Fig. 1a) could be restored by out gassing the sample at 500 K.

UV-Vis spectra were measured in the same cell employed for EPR measurement, so that the results are directly comparable. The UV-Vis spectra of reduced TiAlPO-5 sample before and after ammonia interaction are reported in Fig. 2, (dotted and dashed lines, respectively). For comparison, the spectrum measured on the oxidized sample is also reported (solid curve). Before ammonia interaction the spectra in both oxidized and reduced samples is dominated by a strong absorption at 220 nm, which is typical of ligand-to-metal charge transfer (CT) transitions associated to tetrahedral Ti^{4+} ions, as observed in silica based microporous Ti-silicalite and mesoporous Ti-MCM-41.[6,9,12,27] The assignment of the low energy component at 270 nm, often observed in TiAlPO's structures, is more controversial, since it could be explained both in terms of TiO_x extraframework clusters or of dimeric framework species.[12,19,28] EPR (which is characterized by much higher sensitivity) does not show any clear evidence of clustered TiO_x species, which would resonate at different magnetic fields,[29] supporting the interpretation of the 270 nm band in terms of framework Ti-O-Ti dimers. This assignment is based on the close resemblance with the spectrum of a titanosilsesquioxane model compound, reported by Gianotti et al.,[12] and is validated by the results obtained by pulse ENDOR of O_2^- radical anions (see section 3.2).

Table 1. Spin-Hamiltonian parameters of Ti^{3+} species in TAPO-5 upon different treatments. The parameters are obtained from computer simulations of the CW-EPR spectra in Fig. 1 and Fig. 5. Hyperfine couplings are given in MHz.

Sample	g_x ± 0.001	g_y ± 0.006	g_z ± 0.006								Ref.
Reduced in H_2	1.898	1.918	1.991								This work, (20)
	1.900	1.900	1.969								
Hydrated TiAlPO-5	1.938	1.918	1.865								(20)
TiAlPO-5 + NH_3	1.946	1.913	1.895								This work
	g_x ± 0.0003	g_y ± 0.0003	g_z ± 0.0003	A_x ± 1.5	A_y ± 5	A_z ± 5	a_{iso} ± 5	T_x ± 1.5	T_y ± 5	T_z ± 5	
TiAlPO-5 + $^{17}O_2$	2.0034	2.0099	2.0213	-222.6	-20.3	-17.6	-87	-136	67	70	This work

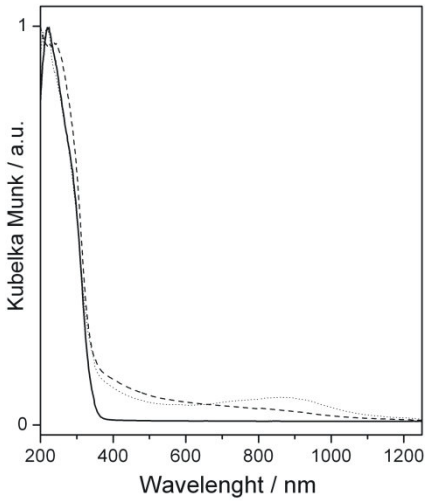

Fig. 2 DR UV-Vis spectra of TiAlPO-5 after oxidation (solid line), reduction (dotted line) and after dosage of 20 mbar of NH_3 (dashed line). Spectra were arbitrarily normalized for easier comparison.

The broad band centered around 870 nm in the reduced sample is ascribed to ligand field *d-d* transition of Ti^{3+} sites in *Td* coordination, formed by reduction of framework Ti^{4+} sites.[20,25] This spectral feature, representing one of the very few examples of electronic spectra of Ti^{3+} ions in tetrahedral symmetry, is in good agreement with the expected $10Dq$ value on the basis of crystal

field theory.[25] After ammonia dosage this band is depleted, with formation of a broad component at higher frequency, similarly to what recently reported in the presence of water molecules.[20] This shift is in agreement with the change in the **g** tensor of the EPR spectrum and consistent with an increase in the crystal field strength, suggesting that NH_3 molecules are entering in the coordination sphere of framework Ti^{3+} ions, as in octahedral $[Ti(H_2O)_6]^{3+}$ complexes, which are characterized by weak bands centred at 500 nm.[25] The change from tetra to hexa-coordination is consistent with the decrease in the intensity of the *d-d* bands. It is well known in fact that *d-d* transitions are Laporte forbidden for octahedral coordination, due to the presence of an inversion centre. On the contrary one order of magnitude intensity gain is observed for tetrahedral geometries due to the absence of an inversion centre and to *d-p* mixing. The insertion of ammonia in the coordination sphere of Ti framework sites is also supported by the change in the high frequency CT absorption, with formation of a component at 240 nm. A similar transformation upon ammonia dosage was reported on Ti-silicalite[27] and Ti-MCM-41[7] and was explained as a CT band from the ammonia ligand to tetrahedral Ti^{4+} centres, confirming their ability to expand their coordination sphere in the presence of adsorbates.

Notice that CT bands, related to Ti^{4+} ions, are characterized by extinction coefficients two/three order of magnitude higher with respect to *d-d* ones, which are instead a fingerprint of Ti^{3+} sites. This fact (and the high intensity of the spectra, close to the limit of application of the Kubelka-Munk function) does not allow to draw conclusions on the fraction of Ti^{4+} ions reducible and able to expand their coordination sphere, on the basis of UV-Vis spectroscopy alone.

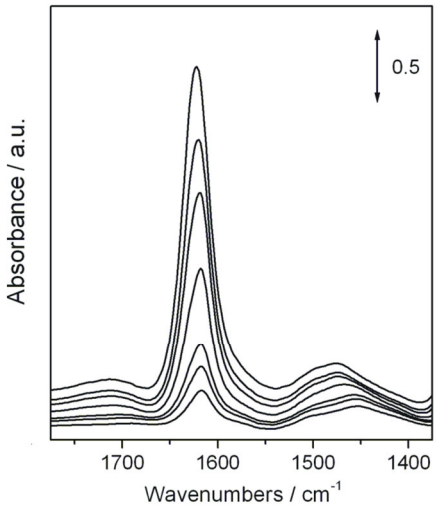

Fig. 3 FTIR spectra of decreasing coverage of ammonia on reduced TiAlPO-5 (higher coverage corresponding to 20 mbar, lower one measured under dynamic out gassing at the IR beam temperature).

Quantitation of reducible Ti ions can however be tackeled by means of EPR by eveluating the amount of Ti^{3+} formed upon reduction. The intensity of the CW-EPR spectrum due to Ti^{3+} ions was monitored at increasing reducing times until the signal intensity was no longer growing. Double integration of the CW-EPR spectra at this stage corresponds to the maximum number of Ti^{3+} species formed upon reduction *i.e.* to the amount of redox active species. Comparing this value with the total amount of Ti incorporated in the sample as determined by ICP analysis (0.7325 ± 0.05%) allow establishing the fraction of reducible framework Ti ions, which is 43±5% of the total icorporated Ti.

Adsorption of ammonia was also followed by FTIR spectroscopy (Fig. 3) monitoring the spectral evolution as a function of ammonia coverage in the N-H bending region. Since the vibrational modes of adsorbed ammonia are quite complex,[30] this region was selected for sake of simplicity. Two main bands are observed, a narrow and intense one at 1622 cm^{-1} with a weaker doublet at 1500 and 1456 cm^{-1}. The latter can be mainly ascribed to the formation of NH_4^+ adducts, mainly formed by proton transfer from mildly acidic surface P-OH groups, as testified by the decrease of the corresponding O-H stretching mode at 3676 cm^{-1} (not reported). On the contrary, the band at 1622 cm^{-1} can be safely assigned to the N-H bending mode of Ti/NH_3 adducts, confirming the Lewis character of the framework Ti centres, which are able to strongly coordinate ammonia molecules.[7,27] These Ti-NH_3 complexes are in fact relatively stable, as they are not completely removed by prolonged outgassing at the temperature of the IR beam. This is consistent with the EPR findings, which show that ammonia displacement occurs by outgassing the sample at 500 K. This temperature is higher than that needed for water displacement (400 K) [20] as expected for the stronger Lewis base (NH_3). Both UV-Vis and FT-IR experiments agree thus with CW-EPR experiments, suggesting that ammonia binds to framework Ti^{3+} ions. Further insights into NH_3 coordination are obtained by means of HYSCORE experiments.

The HYSCORE spectra of NH_3 adsorbed on the reduced TiAlPO-5 sample recorded at magnetic field settings corresponding to the principal *g* values of the field swept EPR spectrum (arrows in Fig. 1b) are reported in Fig. 4 along with the corresponding computer simulations. The spectra are dominated in the (–, +) quadrant by a pair of cross-peaks centered at about (-3.5, 6.9) and

(-6.9, 3.5) MHz, which are assigned to the double-quantum transitions (DQ) arising from the hyperfine interaction of the unpaired electron with a nitrogen nucleus (I = 1). The HYSCORE spectrum of a S = 1/2, I = 1 disordered system is typically dominated by the cross peaks between the DQ frequencies[31]

$$\nu_{dq}^{\alpha,\beta} = 2\sqrt{\left(\frac{a}{2} \pm \nu_I\right)^2 + K^2(3+\eta^2)} \qquad (3)$$

where a is the hyperfine coupling at a given observer position while $K = e^2qQ/4h$ is the quadrupolar coupling constant and η the so called asymmetry parameter. K and η are related to the principal values Q_x, Q_y and Q_z of the traceless **Q** tensor by the following relations: $Q_x = -K(1-\eta)$, $Q_y = -K(1+\eta)$ and $Q_z = 2K$. From Eq. (3) and the position of the DQ cross-peaks, it can be derived a maximum hyperfine interaction of the order of 4 MHz and a quadrupole interaction of the order of 2-3 MHz.

More precise values of these parameters are obtained by means of simulations of the HYSCORE spectra (Fig. 4b and 4d), which were carried out considering a three spin system S=1/2, I_a=1 and I_b=1. Attention was payed not only to reproduce the shape of the DQ peaks, but also to fit the positions of the cross-peaks between the different single-quantum (SQ) frequencies and of the SQ–DQ cross-peaks (see arrows). The observation of the ($-2\nu_\beta^{DQ}$, $2\nu_\alpha^{DQ}$) peaks indicates that at least two virtually equivalent nitrogens, or in other words, at least two NH_3 molecules are binding to Ti^{3+} ions. The complete set of spin-Hamiltonian parameters is listed in Table 2.

Based on the g values extracted from the simulation of the CW-EPR spectrum**,** the unpaired electron can possibly reside either in the d_{xy} or the d_{x2-y2} orbital. Comparison can then be set to the case of nitrogen couplings observed for the molecular complex [1-{2-(*t*-butyl)-2-sila-2,2-dimethyl}-2,3,4,5-tetramethylcyclopentadienyl]-methyl titanium (III),[32] which displays the same EPR g symmetry and axially coordinated nitrogens. The isotropic hyperfine couplings, $|a_{iso}|$ = 4.87 MHz for this system is analogous to that observed in our case (4.1 MHz). The observed isotropic value $|a_{iso}|$=4.1 MHz extracted from the simulation of the HYSCORE spectra, corrsponding to a spin density repartition in the N 2s orbital of 0.0026 (a_{iso} N(2s) = 1540 MHz),[33] is also comparable with values found for nitrogens equatorially bound to an oxovanadium cation, VO^{2+},[34] characterized by a d^1 ground state with the unpaired electron in the d_{xy} orbital.

It should be noted that in the VO^{2+} complexes, the nitrogen hyperfine principal values are negative, due to a spin polarization mechanism.[35] Based on this evidence and assuming a similar ground state for the Ti(III), negative principal values can be expected. On the contrary, the isotropic hyperfine couplings observed for nitrogens coordinated to Cu^{2+} ions (d^9 ground state with the unpaired electron in the d_{x2-y2} orbital)[36] are an order of magnitude larger than those found in our system. This seems to exclude the possibility of a (d_{x2-y2}) ground state in favor of a d_{xy}.

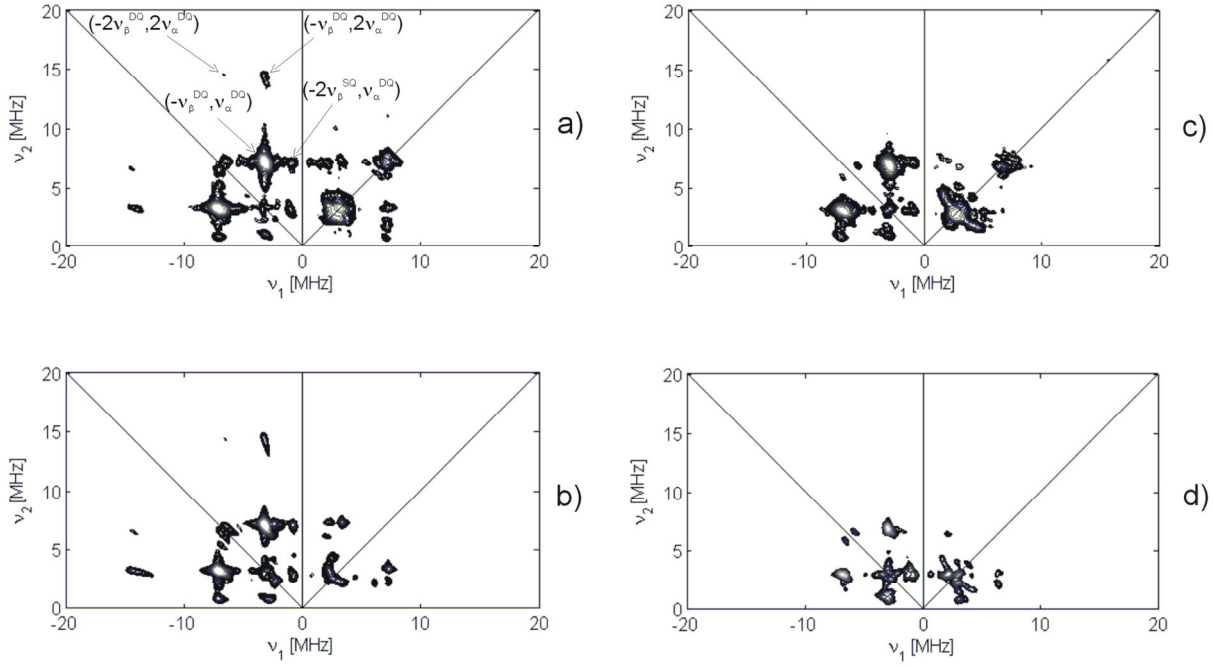

Fig. 4 HYSCORE spectra of reduced TiAlPO-5 in the presence of 20 mbar of NH_3. The spectra are recorded at 7K and taken at observer positions corresponding to a) $g_\perp$ and c)$g_\parallel$. The spectra taken at two τ values (96 and 176 ns) are summed together after Fourier transform. b) and d) Corresponding simulations.

Table 2. ^{14}N hyperfine and nuclear quadrupole values of TiAlPO-5 in the presence of ammonia in comparison with literature results for different Ti^{3+} and VO^{2+} systems containing NH_3 or amine ligands. Hyperfine couplings and quadrupole are given in MHz, the Euler angles are given in degrees.

Sample	$\lvert^N a_{iso}\rvert$	$\lvert^N A_z\rvert$	$\lvert^N A_x\rvert$	$\lvert^N A_y\rvert$	α,β,γ	$\lvert e^2qQ/h\rvert$	α',β',γ	η	*Ref.*
TiAlPO-5	4.1±0.2	3.9±0.2	3.5±0.2	4.8±0.2	0, 90±5, 30±5	2.8±0.1	0, 40±10, 60±10	0.1±0.05	This work
	4.1±0.2	3.9±0.2	3.5±0.2	4.8±0.2	0, 90±5, 30±5	2.8±0.1	0, 40±10, 60±10	0.1±0.05	
C5Me4(CH_2)$_2$NMe_2) TiMe_2	4.4±0.2	3.5±0.2	3.5±0.2	6.2±0.2	90±20	2.3±0.1		0.9±0.1	(26)
VS-1 in SBA-15 / NH_3	4.86±0.05	5.60±0.05	4.40±0.05	4.60±0.05	30±5	2.5±0.1		0.5±0.1	(33)
V-ZSM5 / NH_3	4.8	-	-	-		2-2.32		1-0	(34)

Complementary and important information on the nature of the ammonia binding mode are obtained from the nuclear quadrupole interaction. The electric field gradient described by the parameters e^2qQ/h and η arises primarily from the nitrogen valence 2*p* orbitals, while no contribution is associated to *s* orbitals.[37] For the free NH_3 base, the lone electron pair occupies one of the four sp^3 orbitals with overall C_{3v} symmetry. For such a system an axial electric field gradient is expected, with an asymmetry parameter $\eta = 0$. Crystalline ammonia maintains rigorous axial symmetry (e^2qQ/h= 3.16 MHz, η = 0.0), due to the symmetrical hydrogen bonding pattern in the crystal,[38] while departure of η from zero is associated with asymmetric intermolecular hydrogen bonds. When the ammonia lone pair is shared with an electron acceptor orbital in the Lewis-acid Lewis-base description of bond formation a decrease in the e^2qQ/h value is brought about, while the electric field gradient is expected to remain highly axial after coordination with the metal ion. Indeed in our case we find e^2qQ/h=2.8±0.2 MHz and $0.0<\eta<0.1$. These values agree with those found for amino nitrogens axially ligated to Ti^{3+} in the [1-{2-(*t*-butyl)-2-sila-2,2-dimethyl}-2,3,4,5-tetramethylcyclopentadienyl]-methyl titanium (III) complex[32] and with values obtained for coordination of ammonia to vanadyl sites of vanadium silicate-1 nanoparticles deposited in SBA-15[39] and ZSM-5 zeolites.[40]

3.2 Chemical reactivity of TiAlPO-5 with O_2

Addition of 1.5 mbar of O_2 to the reduced TiAlPO-5 sample leads to the irreversible disappearance of the Ti^{3+} signal of Fig. 1a, which is replaced by a new EPR signal shown in Fig. 1c. This new spectrum is characterized by an orthorhombic powder pattern, characteristic of surface adsorbed superoxide O_2^- species at a single surface site (*i.e.*, one does not observe the simultaneous presence of several groups of O_2^- radicals with different g_z caused by surface heterogeneity). The well resolved superoxide EPR spectrum of $^{16}O_2^-$ is characterized by g_{zz} = 2.023, g_{yy} = 2.010 and g_{xx}=2.003. The **g** matrix is typical for a bound $^2\Pi_{3/2}$ state in which, the local C_{2v} crystal field gives rise to an orthorhombic **g**-tensor with $g_{zz} >> g_{yy} > g_{xx} \approx g_e$ where the *z* direction (largest *g* factor) lies along the internuclear O_2^- axis, and the *x* direction (smallest *g* factor) coincides with the paramagnetic *p* lobes, according to the classical work by Kanzig and Cohen.[41]

The energy splitting between the π^* orbitals (Δ), is caused by the surface crystal field, which in turn directly depends on the charge of the cation onto which O_2^- is adsorbed. Neglecting second-order terms, the resulting value for g_{zz} is $g_{zz}=g_e+2\lambda/\Delta$, where λ is the spin-orbit coupling constant for oxygen. The observed g_{zz} component (2.023) is in nice accordance with earlier literature data[42,43] and typical for an ionic superoxide species stabilized at a Ti^{4+} site.[44,45,46]

Oxygen is a well known electron scavenger and readily reacts with Ti^{3+} via an electron transfer mechanism according to the following equation:

$$Ti^{3+} + O_2 \rightarrow O_2^- + Ti^{4+} \qquad (4)$$

The so formed ionic superoxide (O_2^-) species, at the gas–solid interface, are typically electrostatically adsorbed in either ''end-on'' or ''side-on'' positions. In order to ascertain the adsorption mode of the formed superoxide species, ^{17}O (I=5/2) enriched O_2 was used.

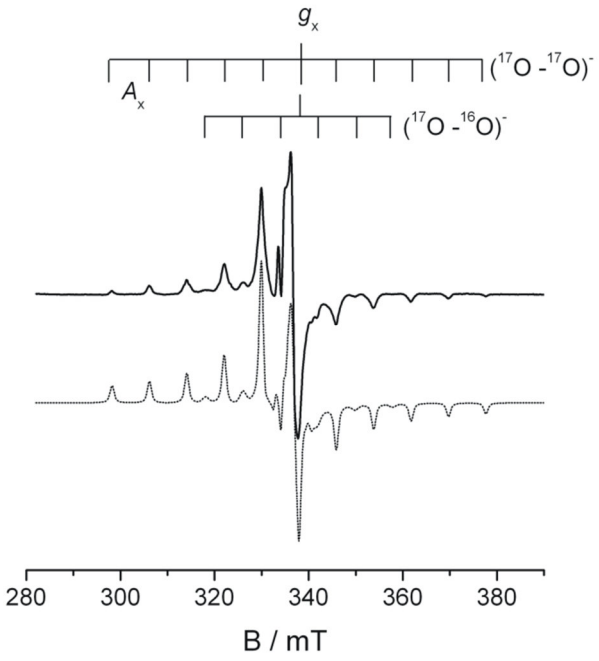

Fig. 5 Experimental (solid line) and simulated (dotted line) CW EPR spectra of $^{17}O_2^-$ adsorbed on reduced TiAPO-5. Spectra were recorded at 77 K. The stick diagrams refer to the two most abundant isotopomers.

The two principal modes of superoxide adsorption corresponding to a "side-on" η^2 structure with equivalent nuclei and a "end-on" η^1 structure with non-equivalent nuclei can be readily distinguished using ^{17}O labeled oxygen.[45]

The case of MgO, where O_2^- radicals are stabilized at the surface with both oxygens magnetically equivalent,[47] and the case of Mo/SiO_2,[48] where they are distinctly non-equivalent, may serve here as good examples.

The spectrum of the $^{17}O_2^-$ radical is shown in Fig. 5 together with its computer simulation. The simulation of the spectrum has been carried out by adding the signals of the three isotopomers $(^{16}O–^{16}O)^-$, $(^{17}O–^{16}O)^-$ and $(^{17}O–^{17}O)^-$ using the same $\boldsymbol{g}$ and $\boldsymbol{A}$ tensors, but weighted by their relative abundance in the gas mixture as determined by the binomial probability ditribution. Since 90% enriched oxygen was used the $(^{17}O–^{17}O)^-$ isotopomer is the dominating species (81% abundance). The spectrum is characterized by a distinct 11 line-pattern arising from the dominant $(^{17}O–^{17}O)^-$ isotopomer, clearly indicating that both nuclei are magnetically equivalent. This finding unambiguosuly implies the formation of a "side-on" η^2 O_2^--Ti^{4+} electrostatic complex. The 11 hyperfine lines are split by approximately 222 MHz. This splitting, corresponding to the ^{17}O A_{xx} hyperfine component, is consistent with other reports for surface adsorbed side-on ionic superoxide species.[47]

The remaining hyperfine tensor components (A_{zz}, A_{yy}) were estimated by computer simulation using as starting values couplings reported for the $^{17}O_2^-$ on MgO.[47] Since these values are not resolved in the spectrum due to the relatively broad line width they are affected by a relatively large error.

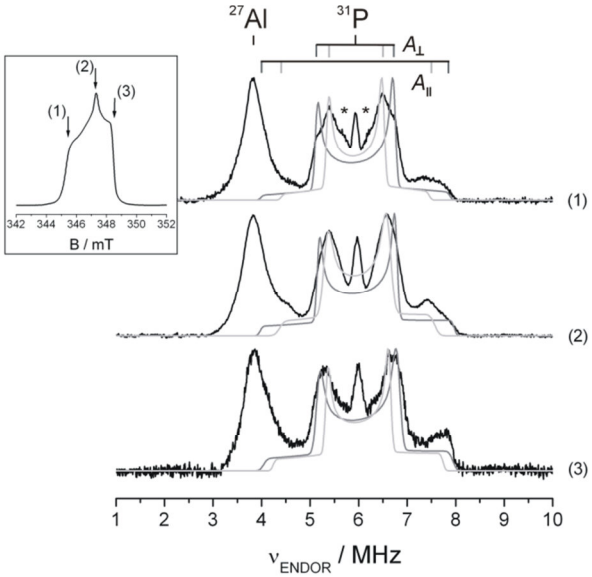

Fig. 6 Experimental (black line) and simulated (grey) ^{31}P Davies ENDOR spectra of TiAlPO-5 upon adsorption of O_2 measured at 10K at 1) 344.4 mT, 2) 346.5 mT and 3) 347.7mT, corresponding to g_z, g_y and g_x features of the echo detected spectrum reported in the inset. The stars indicate a third ^{31}P species (see text).

The rather broad spectral linewidth originates from unresolved hyperfine contributions due to sourrounding magnetically active nuclei (^{31}P, ^{27}Al, ^{1}H) whose contribution can be resolved by means of pulse ENDOR techniques. In particular, further insight into the local environment and localization site of the formed superoxide anion has been obtained by means of pulse ENDOR spectra, which allow monitoring the superhyperfine interactions of the radical anion with nearby magnetic nuclei. ENDOR signals corresponding with interactions between the unpaired electron spin with ^{1}H and ^{31}P nuclei are observed which are described in the following.

3.2.1 ^{31}P Interaction

Davies ENDOR spectra recorded at three different excitation positions in the EPR spectrum, corresponding to the O_2^- principal g values are shown in Fig. 6. The ENDOR powder pattern consists of a number of transitions symmetric with respect to the ^{31}P nuclear Larmor frequency (≈5.97 MHz) having the characteristic shape of a powder pattern due to an axially symmetric tensor. The feature centred at about 4 MHz is due to the contribution of remote Al^{3+} ions and overlaps with the lowest ^{31}P parallel component. Simulation of the spectra were carried out accounting for orientational selectivity during the excitation pulse and are displayed in Fig. 6. The result of the simulation analysis allowed identifying 2 different ^{31}P nuclei with hyperfine couplings listed in Table 3. The choice of the sign of the hyperfine components in Table 3 was made considering the dipolar nature of the O_2^--P hyperfine interaction. In principle the experimental spectrum can be reproduced with the same set of values having all positive signs. This choice was however rejected as it leads to an unrealistically high a_{iso} term, incompatible with a through space hyperfine interaction. Morover the a_{iso} values reported in Table 3 are consistent with values reported for the hyperfine interaction

of oxygen radical species with neighbouring ^{31}P nuclei in apatites.[49]

Two shoulders symmetrically placed with respect to the ^{31}P nuclear Larmor frequency suggest the presence of a third species with hyperfine coupling of the order of 0.8 MHz. The features of this species are largely buried within the spectral linewidth, preventing the determination of the full tensor. A fourth signal centred at ν_P and due to remote phosphorous nuclei is also present, which was not taken into account in the simulation.

Considering a purely dipolar interaction the O_2^--P distance can be estimated to be 0.26-0.27 nm from the following equation:

$$T = \frac{\mu_0}{4\pi} g_e g_n \beta_e \beta_n \frac{1}{r^3} \qquad (5)$$

with r being the distance between the unpaired electron localized in the O_2^- π^* orbitals and the ^{31}P nucleus. Based on this distance and considering that no direct coupling to ^{27}Al ions is detected (only a ^{27}Al matrix line is observed) it is clear that the superoxide radical anion (consistently with the observed g_z factor) is stabilized on the original Ti^{4+} ion substituting for the framework Al^{3+}.

3.2.1 ^{1}H Interaction

Centred at the ^{1}H Larmor frequency a signal with maximum coupling of about 4 MHz is observed due to a ^{1}H interacting with the O_2^- radical.

Pulse ENDOR spectra recorded with the Mims sequence at magnetic field settings corresponding to the principal **g** tensor values are shown in Fig. 7. The spectra can be simulated considering an axially symmetric tensor dominated by a dipolar interaction with T = 2.0±0.2 MHz, corresponding to a O_2^-—H distance of approximately 0.34±0.01 nm. A broad line-width (0.75 MHz) was used in the simulation indicating the presence of a conformational heterogeneity, as may be expected due to the polycrystalline nature of the sample. As in the case of the ^{31}P coupling a sharp peak at the ^{1}H Larmor frequency is present due to remote (matrix) protons.

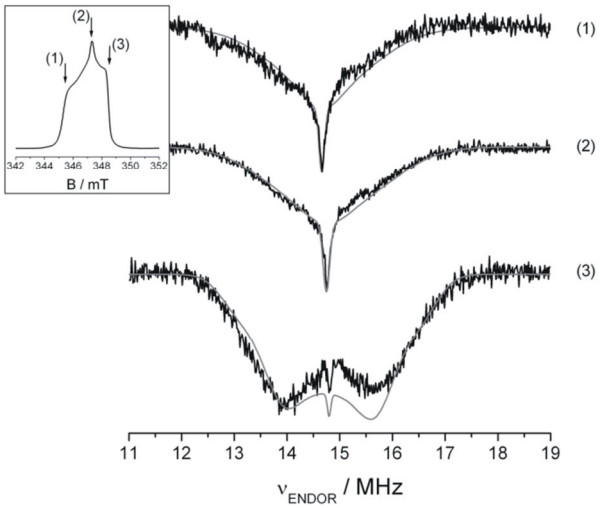

Fig. 7 Experimental and simulated (grey line) ^{1}H Mims ENDOR of O_2^- ions in TiAlPO-5 recorded at field positions corresponding to the EPR powder spectrum turning points (field positions indicated in the inset). Each spectrum is the sum of several spectra recorded at different τ values. All spectra were measured at 10K.

The O_2^--H distance derived from the ENDOR spectrum excludes that the proton is stabilized on the nearest oxygen, while is consistent with the presence of an OH^- group in the second oxygen coordination sphere of the original Ti^{3+} ion as shown in Scheme 1d.

The presence of a proton can be rationalized considering the TiAlPO-5 reduction mechanism and the electro neutrality of the system. ^{31}P HYSCORE spectra of H_2 reduced TiAlPO-5 provided in fact a unique and direct proof for framework substitution of Ti^{3+} for the isovalent Al^{3+}.[20] Based on this evidence we proposed a mechanism for the incorporation of Ti ions which involved the substitution of an Al^{3+} and P^{5+} pair by two Ti^{4+} ions,[20] similarly to the well known mechanism for incorporation of Si in SAPO materials (Scheme 1a,b).[50] Upon reduction of the sample with H_2 (Scheme 1c), Ti^{3+} ions are formed replacing for isovalent Al^{3+} ions, while a proton, stabilized nearby a Ti^{4+} at a P^{5+} position, will grant the electro neutrality of the system. Based on this scheme the maximum amount of reducible Ti will be 50% of the total incorporated Ti corresponding to those Ti ions replacing for Al^{3+} ions. The experimental value of 43% found experimetally thus indicates that this mechanism is indeed the dominant one.

For the sake of electro neutrality, the two Ti ions do not need to be nearest neighbours, however the observation of the O_2^--H interaction at a distance of about 0.34 nm clearly proves that Ti-O-Ti pairs are formed. The O_2^- g_z factor and ^{31}P hyperfine couplings demonstrate that the superoxide formed upon reaction of reduced TiAlPO-5 with molecular oxygen is stabilized on a Ti ion originally replacing for an Al^{3+}. Detection of the ^{1}H coupling reported in Table 3, on the other hand, is only compatible with a

second Ti ion, substituting for a P^{5+} ion at a next neighbour position forming a Ti-O-Ti oligomer. This model is perfectly matching with the interpretation of UV-Vis spectra (see above), suggesting that the presence of a component at 270 nm in TiAlPOs samples can be interpreted as a unambiguous fingerprint for framework Ti-O-Ti moieties.

Table 3. ^{1}H and ^{31}P hyperfine values of TiAlPO-5 upon adsorption of O_2. Hyperfine couplings are given in MHz, the Euler angles are given in degrees.

	A_x ± 0.2	A_y ± 0.2	A_z ± 0.1	a_{iso} ± 0.05	T_x ± 0.2	T_x ± 0.2	T_x ± 0.2	β ± 2
^{1}H	-2.2	-2.2	4.0	-0.13	-2.07	-2.07	4.14	90
	-0.01	-0.01	0.02	0	-0.01	-0.01	0.02	90
^{31}P	-1.65	-1.65	4.0	0.23	-1.88	-1.88	3.76	90
	-1.3	-1.3	3.5	0.3	-1.6	-1.6	3.2	90

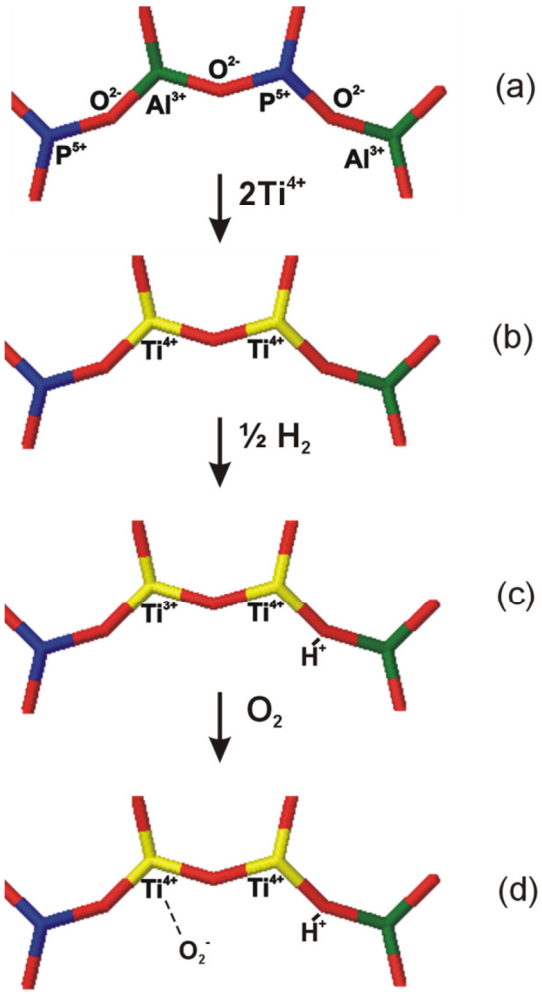

Scheme 1. Schematic representation of the Ti insertion and subsequent reactivity with oxygen of TiAlPO-5.

We note that failure to detect this ^{1}H coupling in the HYSCORE spectrum of reduced TiAlPO-5[20] may be due to suppression effects induced by the strong ^{31}P and ^{27}Al modulations and failure to record pulse ENDOR spectra because of the fast relaxations of Ti^{3+} ions.

4. Conclusions.

The reactivity of reduced TiAlPO-5 towards ammonia and molecular oxygen was studied by means of CW EPR and pulse EPR and ENDOR methods and complementary UV-Vis and FT-IR spectroscopies. The results reported can be summarized as follows: 1) Ti^{3+} ions are formed upon reduction with H_2 at framework positions substituting for Al^{3+} ions. The fraction of reducible Ti ions corresponds to 43% of the total incorporated Ti strongly suggesting that Ti ions enter the framework in pairs substituting for Al^{3+} and P^{5+} couples; 2) the Ti^{3+} sites are coordinatively unsaturated and capable of reversibly coordinating two ammonia molecules as

detailed by means of HYSCORE spectroscopy; 3) the same sites undergo an electron transfer reaction towards molecular oxygen leading to the formation of superoxide radical anions; 4) pulse ENDOR spectra reveal that the superoxide radical is stabilized on the redox active Ti ions at Al^{3+} framework positions and interacts with a proton at a distance of 0.34±0.01 nm. This can be explained only considering the formation of Ti-O-Ti oligomers. This in turns validates the interpretation of the UV-Vis component at 270 nm in TiAlPOs materials as a fingerprint of framework Ti-O-Ti moieties.

These results represent an important advancement in the understanding of the Ti incorporation mechanisms in AlPO materials and promise to be relevant in tuning of the activity and selectivity of the catalyst to the desired reaction.

Notes and references

[a] *Dipartimento di Chimica IFM, Università di Torino and NIS, Nanostructured Interfaces and Surfaces Centre of Excellence, Via P. Giuria 7, I - 10125 Torino, Italy. E-mail: m.chiesa@unito.it*

[b] *Present address: Laboratoire Catalyse et Spectrochimie, UMR CNRS 6506, ENSICAEN and Université de Caen Basse-Normandie, 6 Boulevard du Maréchal Juin, 14050 Caen Cedex, France.*

[1] G. Bellussi, A. Carati, G. M. Clerici, G. Maddinelli and R. Millini, *J. Catal.,* 1992, **133**, 220; B. Notari, *Adv. Catal*., 1996, **41**, 253.
[2] I. Arends, R. A. Sheldon, M. Wallau and U. Schuchardt, *Angew. Chem. Int. Ed. Engl.,* 1997, **36**, 1144.
[3] R. D. Oldroyd, G. Sankar, J. M. Thomas and D. Ozkaya, *J. Phys. Chem. B,* 1998, **102**, 1849.
[4] A. Corma, M. T. Navarro and J. Pérez Pariente, *J. Chem. Soc.,Chem. Commun.*, 1994, 147.
[5] R. D. Oldroyd, J. M. Thomas, T. Maschmeyer, P. A. MacFaul, D. W. Snelgrove, K. U. Ingold and D. D. M. Wayner, *Angew. Chem., Int. Ed. Engl.*, 1996, **35**, 2787.
[6] T. Maschmeyer, F. Rey, G. Sankar and J. M. Thomas, *Nature*, 1995, **378**, 159.
[7] E. Gianotti, V. Dellarocca, L. Marchese, G. Martra, S. Coluccia and T. Maschmeyer, *Phys. Chem. Chem. Phys.*, 2002, **4**, 6019.
[8] M. Anpo and J. M. Thomas, *Chem. Commun.*, 2006, 3273.
[9] A. Zecchina, S. Bordiga, C. Lamberti, G. Ricchiardi, D. Scarano, G. Petrini, G. Leofanti and M. Mantegazza, *Catal. Today,* 1996, **32**, 97.
[10] S. Bordiga, F. Bonino, A. Damin and C. Lamberti, *Phys. Chem. Chem. Phys*, 2007, **9**, 4854.
[11] G. Sankar, J. M. Thomas, C. R. A. Catlow, C. M. Barker, D. Gleeson and N. Kaltsoyannis, *J. Phys. Chem. B*, 2001, **105,** 9028-9030.
[12] E. Gianotti, A. Frache, S. Coluccia, J. M. Thomas, T. Maschmeyer and L. Marchese, *J. Mol. Catal. A*, 2003, **204**, 483.
[13] S. Bordiga, A. Damin, F. Bonino, G. Ricchiardi, C. Lamberti and A. Zecchina, *Angew. Chem. Int. Edit.*, 2002, **41**, 4734.
[14] J. To, A. A. Sokol, S. A. French and C. R. A. Catlow, *J. Phys. Chem. C,* 2008, **112**, 7173.
[15] A. Gamba, G. Tabacchi and E. Fois, *J. Phys. Chem. A*, 2009, **113**, 15006.
[16] P. E. Sinclair, G. Sankar, C. R. A. Catlow, J. M. Thomas and T. Maschmeyer, *J. Phys. Chem. B*, 1997, **101**, 4232.
[17] S. T. Wilson, B. M. Lok, C. A. Messina, T. R. Cannan and E. M. Flanigen, *J. Am. Chem. Soc.*, 1982, **104**, 1146.
[18] S. O. Lee, R. Raja, K. D. Harris, J. M. Thomas, B. F. G. Johnson, G. Sankar, *Angew. Chem. Int. Ed.*, 2003, **42**, 1520.
[19] J. Paterson, M. Potter, E. Gianotti and R. Raja, *Chem. Commun.* 2011, **47**, 517.
[20] S. Maurelli, V. Muthusamy, M. Chiesa, G. Berlier, S. Van Doorslaer, *J. Am. Chem. Soc.*, 2011, **133**, 7340.
[21] P. Höfer, A. Grupp, H. Nebenführ and M. Mehring, *Chem. Phys. Lett.*, **1986**, *132*, 279.
[22] S. Stoll and A. Schweiger, *J.Magn.Reson*. 2006, **178**, 42.
[23] A. Tuel, J. Diab, P. Gelin, M. Dufaux, J. F. Dutel and Y. B. Tarit, *J. Mol. Catal.* 1990, **63**, 95.
[24] A. M. Prakash, H. Mi Sung-Suh and L. Kevan, *J. Phys. Chem. B*, 1998, **102**, 857.
[25] B. N. Figgis, *Introduction to Ligand Fields*, John Wiley & Sons Eds: New York, 1967.
[26] J. A. Weil, J. R. Bolton and J. E. Wertz, *Electron Paramagnetic Resonance: Elementary Theory and Practical Applications*; John Wiley: New York, 1994, 213.
[27] S. Bordiga, S. Coluccia, C. Lamberti, L. Marchese, A. Zecchina, F. Boscherini, F. Buffa, F. Genoni, G. Leofanti, G. Petrini and G. Vlaic, *J. Phys. Chem.*, 1994, **98**, 4125.
[28] M. H. Zahedi-Niaki, M.P. Kapoor and S. Kaliaguine, *J. Catal*., 1998, **177**, 373.
[29] R.F. Howe, M. Graztel, *J. Phys. Chem.*, 1985, **89**, 4495.
[30] A. Zecchina, L. Marchese, S. Bordiga, C. Paze and E. Gianotti, *J. Phys. Chem. B*, 1997, **101**, 10128.
[31] S. A. Dikanov, Y.-D. Tsvetkov, M. K. Bowman and A. V. Astashkin, *Chem. Phys. Lett*., 1982, **90**, 149.
[32] S. Van Doorslaer, J. J. Shane, S. Stoll, A. Schweiger, M. Kranenburg and R. J. Meier, *J. Organomet. Chem.*, 2001, **634**, 185.
[33] J. A. J. Fitzpatrick, F. R. Manby and C. M. Western, *J. Chem. Phys*, 2005, **122**, 084312.
[34] K. Fukui, H. Ohya-Nishigchi and H. Kamada, *Inorg. Chem.*, 1997, **36**, 5518; C. Buy, T. Matsui, S. Andrianambinintsoa, C. Sigalat, G. Girault and J. L. Zimmermann, *Biochemistry*, 1996, **35**, 14281; K. Fukui, H. Ohya-Nishigchi, H. Kamada, M. Iwaizumi and Y. Xu, *Bull. Chem. Soc. Jpn.*, 1998, **71**, 2787; S. A. Dikanov, A. M. Tyryshkin, J. Hüttermann, R. Bogumil and H. Witzel, *J. Am. Chem. Soc.*, 1995, **117**, 4976; S. A. Dikanov, R. I. Samoilova, J. A. Smieja and M. K. Bowman, *J. Am. Chem. Soc.*, 1995, **117**, 10579; C. F. Mulks, B. Kirste, H. Van Willigen and M. K. Bowman, *J. Am. Chem. Soc.*, 1982, **104**, 5906; B. Kirste and H. Van Willigen, *J. Phys. Chem.*, 1982, **86**, 2743.
[35] C. P. Scholes, K. M. Falkowski, S. Chen and J. Bank, *J. Am. Chem. Soc.*, 1986, **108**, 1660.
[36] T. G. Brown and B. M. Hoffman, *Mol. Phys.* 1980, **39**, 1073. S. P. Greiner, D. L. Rowlands and R. W. Kreilick, *J. Phys. Chem.*, 1992, **96**, 9132.
[37] C. H. Townes and B. P. Dailey, *J. Chem. Phys.*, 1949, **17***,* 782.
[38] S. S. Lehrer and C. T. O'Konski, *J . Chem. Phys.*, 1965, **43**, 1941.
[39] S. Zamani, M. Chiesa, V. Meynen, Y. Xiao, B. Prélot, J. Zajac, F. Verpoort, P. Cool, P. and S. Van Doorslaer, *J. Phys. Chem. C*, 2010**, 114***,* 12966.
[40] J. Woodworth, M. K. Bowman and S. C. Larsen, *J. Phys. Chem. B*, 2004, **108**, 16128.
[41] W. Kanzig, and M. H. Cohen, *Phys. Rev. Lett.*, 1959**, 3**, 509.
[42] A. M. Prakash, V. Kurshev and L. Kevan, *J. Phys. Chem. B*, 1997, **101**, 9794.
[43] K. L. Antcliff, D. M.Murphy, E. Griffiths and E. Giamello, *Phys. Chem. Chem. Phys*., 2003, **5**, 4306.

[44] Z. Sojka, *Catal. Rev. Sci. Eng*., 1995, **37**, 461.
[45] M. Che and A. J. Tench, *Adv. Catal*., 1983, **32**, 1.
[46] F. Geobaldo, S. Bordiga, A. Zecchina, E. Giamello, G. Leofanti and G. Petrini, *Catalysis Lett*., 1992, **16**, 109.
[47] M. Chiesa, E. Giamello, M. C. Paganini, Z. Sojka and D.M. Murphy, *J. Chem. Phys*., 2002, **116**, 4266.
[48] E. Giamello, D. M. Murphy, E. Garrone and A. Zecchina, *Spectrochim. Acta*, 1993, **49**A, 1323.
[49] S. Van Doorslaer, P. Moens, F. Callens, P. Matthys and R. Verbeeck, *Appl. Mag. Reson.,* 1986, **10**, 87.
[50] H. O. Pastore, S. Coluccia and L. Marchese, *Annu. Rev. Mater. Res*., 2005**, 35**, 351.